Elucidating the role of soil hydraulic properties on ~~the~~ aspect-dependent landslide initiation

Yanglin Guo[1, 2], Chao Ma[1, 2]

1. School of Soil and Water Conservation, Beijing Forestry University, Beijing 100083, PR China.

2. Jixian National Forest Ecosystem Observation and Research Station, CNERN, Beijing Forestry University, Beijing 100083, PR China.

Corresponding Author~~to~~: Professor Chao Ma, sanguoxumei@163.com

Abstract: Aspect-dependent landslide initiation is an interesting finding, and previous studies have attributed this ~~observation~~ to the mechanical effects of plant roots. In the pre~~i~~sent study~~work~~, an overwhelming landslide probability on a south-facing slope over a north-facing slope was found in a localized area with on~~mere~~ly granite underneath and high cover of *Larix k~~K~~aemp~~h~~feri* ~~species~~. These~~Such~~ observations cannot be~~not~~ attributed to plant roots~~,~~ but may result from factors related to hillslope hydrology~~the hillslope hydrology related factors~~. D~~The d~~ifferential weathering ~~-~~associated with hillslope hydrology behaviors~~,~~ such as rainfall water storage and leakage, pore water pressure, particle component, and hillslope stability fluctuation~~,~~ were used to elucidate these ~~such~~ observations. Remote sensing interpretation using the high-resolution GeoEye-1 image and digitalized topography showed~~revealefound~~ that ~~the~~ landslides on south-facing slopes have a higher probability, larger basal area, and shallower depth than those on a north-facing slope. The lower limits of the upslope contributing area and slope gradient condition for south-facing landslides were~~is~~ less than those for north-facing landslides. The higher basal areas of south-facing landslides than those of the~~over~~ north-facing landslides may be attributed to the high peak values and slow dissipation of pore water pressure. The absorbed and drained water flow in a given time interval, together with the calculated water storage and leakage during the measured rainy season measured, demonstrate~~, sufficiently prove~~ that the soil mass above the failure zone for ~~the~~ south-facing slopes is~~are~~ more prone to ~~form~~ pore-water pressure, which~~and~~ results in slope failures. In comparison, the two stability fluctuation results from the finite and infinite models further verified that landslides on south-facing slopes may fail under~~on~~ conditions of prolonged antecedent precipitation and intensive rainfall.~~,~~ Meanwhile,~~whereaswhile~~ those on north-facing slopes may fail on~~mere~~ly in response to intensive rainfall. The results of this study will deepen our knowledge of~~work~~ ~~provide an insightful view ofn the~~ aspect-dependent landslide initiation from both classical mechanics and the state of stress.

Keywords: Landslide; Pore pressure; suction stress; Hydraulic conductivity; Slope stability

1 Introduction

In some semi-arid environments of the Northern H~~h~~emisphere, aspect-dependent landslide initiation ~~would~~ provides valuable insights into the relative importance of different factors in developing accurate landslide susceptibility models (Ebel, 2015; Rengers et al., 2016; Li et al., 2021; Deng et al., 2022). These events provide a thorough~~tful~~ understanding of~~about~~ the amount of direct sunlight that translates into differences in vegetation communities~~y~~, bedrock weathering, and soil development processes (Fu, 1983; Wang, 2008; Bierman and Montgomery, 2014). These ~~typical~~ earth surface processes indirectly affect hillslope hydrology and landscape dissection at~~on~~ the hillslope scale. ~~Importantly,~~ R~~r~~ainfall-induced shallow landslides are ~~one of the~~ geomorphic agents at~~on~~ the hillslope scale and are governed by multiple factors, including hydrology, hillslope materials, bedrock ~~underneath~~, and ~~the~~ vegetation (Birkeland, 1999; Geroy et al., 2011; Lu and Godt, 2013). Currently, the ~~observed~~ aspect-dependent landslide initiation observed has been predominantly~~is mainly~~ attributed~~s~~ to the mechanical effect of plant roots. This is~~,~~ because the differences in~~of~~ vegetation on the south- and north-facing slopes are easier to examine and more pronounced ~~obvious~~ than other factors (Li et al., 2021; Timilsina et al., 2021; Dai et al., 2022; Deng et al., 2022). However, ~~it is no denying that~~ vegetation succession takes place over substantially longer timescalesis far slowly than_ the soil development and bedrock weathering (Watakabe and Matsushi, 2019)., In most cases,and the plantir roots arein most cases is not deep enough to penetrate into the bedrock (Schwinning, 2010). Hypothesizing forin a relatively localized area with the same ecosystem or plant species, aspect-dependent landslide initiation cannot benot attributed to plant roots, butwhile may result from the differences in the properties of hillslope materials due to long-term differential weathering.

AThe aspect-dependent landslides in the Frontal Colorado, USA and the Loess Plateau, China, have attracted interest because vegetation hasinteresting focus that vegetation generates a considerable influence on the landslide distribution. TheIn fact, the strong overwhelming propensity for shallow landslide initiation on south-facing hillslopes in the two regions is closely relateds to the present -day tree density, regardless of the hillslope aspect (Ebel, 2015; Rengers et al., 2016; Deng et al., 2022). In the Colorado Frontal Range, field observations have shownproved that south-facing slopes lack thick tree cover and have an abundance of rock outcrops compared to north-facing slopes., In addition,and the soil layer iswould be thinner on south-facing slopes (Coe et al., 2014; Ebel et al., 2015). The apparent cohesion supplied by the roots iwas responsible for the observed connection observed between landslide distribution and slope aspect (McGuire et al., 2016). OnIn the Loess Plateau China, vegetation recovery is one of the main athe major ecological measures for mitigatingto mitigate the sediment loss (Fu et al., 2009). IncreasedPromoted soil strength and hydraulic conductivity due to strong root networks may enhance the the topographic initiation conditions (Montgomery and Dietrich, 1994; Wang et al., 2020). Another possibility is that the Nnorth- and west-ward moving storms may potentially produce produced more intense rainfall on the south- and east--facing slopes. Such an This assumption may be invalid if an aspect-dependent landslide distribution is presentexists in a localized catchment with a specificgiven vegetation communityies. TheIn fact, the above-mentioned This study highlights the effect of the mechanical function of plants on landslides. If anthe aspect-dependent landslide exists in a localized area that are with vegetation cover comprisingcovered by the same plant species alongside a high level ofand high vegetation coverage, the observed aspect-dependent landslide initiation observed cannot benot attributed to the mechanical effect offrom plant roots.

To determine elucidate the observed relationship observed among vegetation, landslides, and slope aspect, the effects offrom the physical properties and strength of hillslope materials cannot be excludedignored. OnIn the nNorthern part of the Loess Plateau, China, as well as in many other semi-arid environments, different types and densities of vegetation and soils develop on north-facing versus south-facing convergent slopes. This is, because systematic differences in the amount of direct sunlight translate into differences in the physical and chemical weathering. North-facing convergent slopes have lower evaporation rates, retain snow cover longer in spring, and tend to hold soil moisture longer duringto the summer growing season. TheseSuch differences may result in localized ecosystem communities in the presence of trees or shrubs onover grasses. South-facing slopes experience heavier and more frequent hydration, thermal expansion, or freeze-thaw cycles due toby the day warming and night cooling, and tend to havefavor stronger weathering throughout the year. Such These differences can could result in local differences in the grain component, soil strength, and soil profile., This has indirect effects atwhich indirectly affect the landslide scale throughby the mechanics of excessive pore water pressure dissipation and sliding surface liquefaction (Terzaghi, 1950; Sassa, 1984), and the hillslope hydrology behavior (Godt et al., 2009; Lee and Kim, 2019). Therefore, the physical properties of the hillslope materials may be attributed to the observed aspect-dependent landslide initiation observed.

It is well known thatAs known to Aall, shallow landslides are anone of the examples of debris flow initiation, which often enlarges their scale by multiple mechanics (Hungr et al. 2005; Iverson et al. 2011). When the slope fails, the pore water pressure abruptly increases within the shear zone (Iverson and LaHusen, 1989; Wang and Sassa, 2003). If the excessive pore water pressure persists high over the static pressure for a relatively long duration, the displaced masses will enlarge their volume by widespread liquefaction, and transform into debris flows (Bogaard and Greco, 2016). ~~In other words,~~ T~~t~~he magnitude of the pore water pressure is closely related~~s~~ to the scale of the shallow landslide. Therefore, the scale of ~~the~~ shallow landslides can~~could~~ be determined ~~elucidated~~ by the role of excessive pore water pressure during the failure process. However, the aspect-dependent landslide distribution in these ~~the~~ two ~~above mentioned~~ areas ~~merely~~ refers to the differences in landslide probability rather than ~~and, not~~ the landslide scale.

In the pre~~i~~sent study~~work~~, we used a combination of field soil moisture observation, strength measurement, ~~and~~ hydraulic conductivity analysis of hillslope materials, and numerical modeling of slope stability to explain the high potential for ~~the overwhelming~~ landslide initiation on south-facing slopes relative to north-facing slopes with the same~~,~~ ~~where the~~ vegetation communities ~~are the same~~. ~~In addition, the~~ D~~d~~ifferences in landslide geometry and initiation conditions, in the form of the contributing area above the scar area and the landslide gradient, were shown using ~~exhibited by the~~ field studies ~~investigations~~ and high-resolution GeoEye-1 images. ~~Then,~~ T~~t~~he differential weathering-related physical properties and strength of the soil mass, including the dry unit weights, porosity, ~~and~~ grain size, effective cohesion, and inner friction angle~~,~~ were examined. ~~Importantly,~~ W~~w~~e have also highlighted the importance of ~~the~~ excessive pore water pressure, hillslope hydrology, and stability in~~to~~ explaining the ~~observed~~ aspect-dependent landslide initiation observed. The results of this work will deepen our ~~may provide an insightful~~ understanding of ~~the~~ aspect-dependent landslide distribution in some mountainous areas of the Northern H~~h~~emisphere.

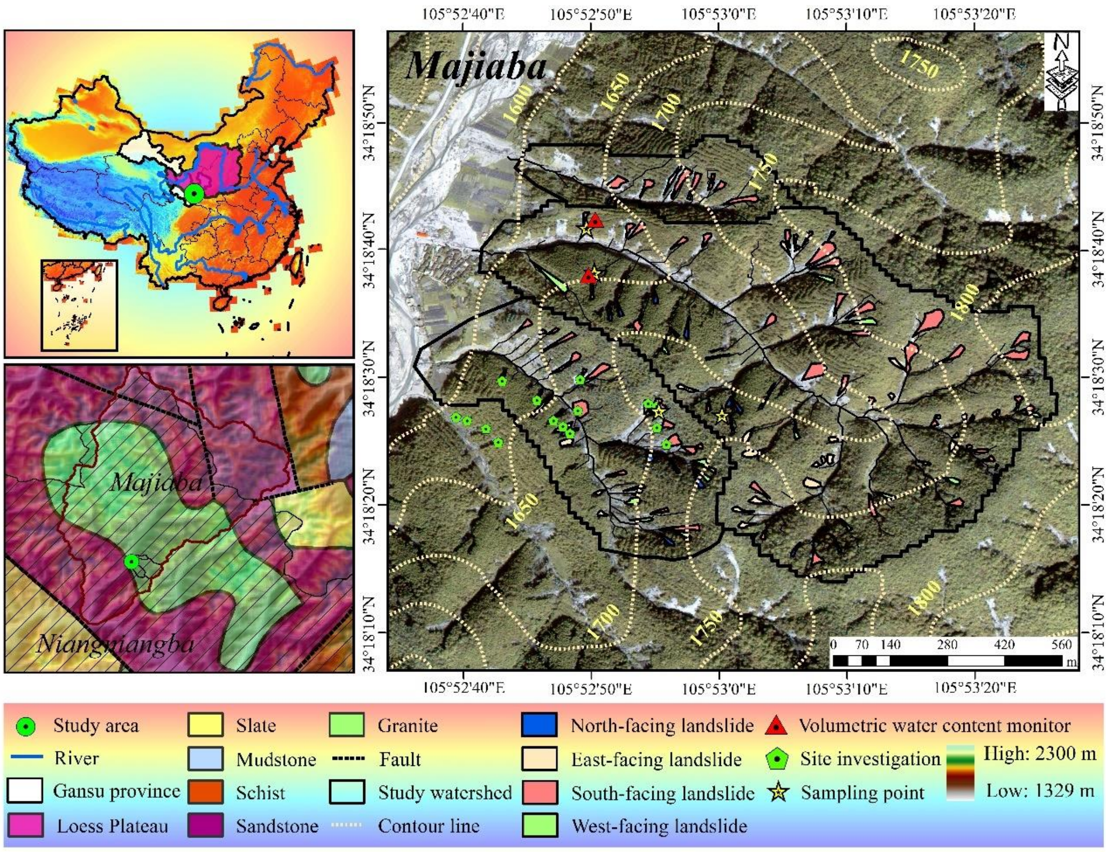

Fig. 1. Location, topography, and simplified lithology of the study area. ~~(~~All maps are created by the authors. The graph of Majiaba was taken using~~by~~ an Unmanned Aerial Vehicle. The territorial domain of China and simplified lithology map are from China Geological survey.~~)~~

2 Study area

The study area is in the mountainous region of Majiaba village ~~in, the~~ northeast of Niangniangba town, Tianshui

City, Gansu Province, Central China. It is also close to the dividing crest of the Yellow River and Yangtze Rivers, and onin the eastern part of the Loess Plateau. The mMajority Most of the hillslope isare underlain by slate,; and the stratigraphic units of granite, sandstone, and mudstone account for a relatively smaller area. This area in semi-humid climate region and has four distinctive seasons andin a semi-humid climate. The annual precipitation is approximately 491.6 mm and predominantly falls mostly falls during June and August. One branch fault of the Tianshui–-Lanzhou fault system runs through the area and has had no rupture records for the last few decades.

The shallow landslides in the study area and nearby surroundings were triggered by the prolonged antecedent precipitation during July 1–241 to 24 July and the intensive rainstorm on 25 July 25, 2013 (Yu et al., 2014; Guo et al., 2015). Previous studies found that majority of Most shallow landslides in the entirewhole storm-spanned the mountain area with ahave gradient of 20–25 °, located on south-facing slopes and in areas with relatively sparse vegetation (Li et al., 2021). In additionBesides, Tthehe strong root network may promote the hydraulic conductivity of the soil–-root composite and the landslide initiation condition of the upslope contributing area–-slope gradient, according to the landslide case studiess fromin the *Larix kKaemphferi* and *Pinus tabuleaformis* forests (Dai et al., 2022). In this studywork, Tthe three small catchment areas in the Majiaba Wwatershed areweare underlain by granite units. The total area is 0.88 km^2 with vegetation cover coverage rate of over 90% (Fig. 1). The relative relief wais approximatelyabout 200 m, and the mean hillslope gradient wais 37°. The reasons why choose the three catchments lie in the area were chosen is that the main plant species on the south- and north-facing slope is *Larix kKaemphferi*, which commonly have highly-developedhighly developed lateral roots with depth < 0.4 m. However, landslides in the three catchments still have a higher exhibit overwhelm propensity for occurrence onon south-facing slopes in comparison with the over north-facing slopes. ThisSuch a finding differentiates from the results fromin the Frontal Colorado, USA, and the Central Loess Plateau,; where landslides commonly occur in sparsely vegetated areas. Furthermore, the works of Li et al. (2021) only merely addressed the relationship between landslide probability and vegetation cover at the coverage oin a regional scale, while excluding neglectinged the importance of the properties of hillslope materials atin a more localized scale. Therefore, we hypothesize that such observations in the study area may not be the result of from the mechanical effect of plant roots, but may be from the distinctive physical properties and strength of hillslope materials due to differential weathering.

3 Materials and methods

3.1 Landslide information interpretation

The high -resolution (0.5 m × 0.5 m), on October 8, 2013). The GeoEye-1 image was orthorectified and the landslide boundary was visually interpreted usingby ENVI 5.1 and e-Cognition 8. An unmanned aerial vehicle (UAV for abbreviation) was used to obtain athe digital elevation model (DEM) with a 5 m resolution. The GeoEye-1 orthographic image and DEM were spatially registered in the ArcGIS 10.2 as aby standard layer of orthoimage. The landslide initiation condition is represented by the competition between the slope gradient and the upslope contribution area (A–-S):

$$S = kA^{-b} \tag{1}$$

where S is the local slope (m/m); A is the contribution area above the landslide head -scar (m^2); k is an empirical constant, which is related to lithology, vegetation, and climate; and b is an empirically defined index.

Field studies investigations werewere conductedmainly to measure the depth of the head -scar and sidewall area usingby tape, and the failure depth wais taken as their average of them. Then, the landslide volume could thenan then be calculated usingby the interpreted scar area and the measured the depth. measured. Finally, Ddetailed landside information, including the landslide number and area probability, landslide volume and width, head -scar and sidewall depth, andas well as the upslope contributing area–-slope gradient condition for the south- and north-facing slopes were compared.

3.2 Field monitoring and soil sampling

To investigate the hillslope hydrology on the south- and north-facing slopes, the Frequency Domain Reflectometry (FDR) soil moisture sensors were used in this work to record the volumetric water content. To avoid the randomness of data caused by natural factors such as terrain and vegetation, a total of 16 shallow landslides were investigated, to excavate soil profiles and take undisturbed soil samplesing. Then, the Ssensors were installed implemented at depths of 30 cm, 70 cm, and 110 cm on the south- and north-facing slopes, to monitor the volumetric water content during the rainy season of 2021. SThe soil moisture monitoring was implemented atworks were implemented on two concave sites on the south- and north-facing slopes. The meteorological station wais less no more than 3 km away from the study area to record the rainfall on a 30 min basis. During the sensor installations implementation, the undisturbed soil sampleings near the sensor location were taken for indoor tests, including the dry unit weight, porosity, grain size, shear strength, and hydraulic conductivity. The grain size was analyzed using aby Malvern MS 3000 instrument (Malvern, England). In each layer, at least four4 samples weare collected for the consolidated undrained triaxial compression test (CU)., Tand two2 samples were collected for unsaturated hydraulic conductivity measurement usingby transient release and imbibition method tests (Lu and Godt, 2013). Saturated hydraulic conductivity was determined using the constant water head method (Table 1).

3.3 Pore water pressure dissipation

CU tests werWe performed CU tests to obtain the effective cohesion, effective internal friction angle, and the pore pressure water dissipation curves. SThe soil samplesing, with a diameter of 50 mm and height of 100 mm, were firstly saturated in a vacuum pump. They wereand, then consolidated in the chamber of the GDS apparatus atby 50, 100, 150, and 200 kPa confining pressures and 10 kPa backpressure. During each test, the shearing rate was set toas 0.1 mm/min, and the device automatically recordedrecords one data every 10 s. Owing to the varied particle components and soil texture, the increasing and dissipation ratios variedyies. Furthermore, Ththis ratio is closely relatedsuch ratio closely relates to the widespread generation of excessive pore-water pressure, which increaseswill enlarge the landslide scale. A hHigh excessive pore water pressure, rapid increase ratio, and slow dissipation ratio could cause widespread Ceoulomb failure within the sliding zone. To demonstrate thatshow the pore water pressure increases or dissipates, the ratio is:

$$i = \frac{p_{t+\Delta t}-p_t}{\Delta t} \qquad (2)$$

where i is the increase or dissipation ratio of the excessive pore water pressure, and p_t and $p_{t+\Delta t}$ are the measured pore water pressures measured during the time interval of Δt.

3.3 Water storage and drainage

The unsaturated permeability of soil mass (diameter 61.8 mm, height 25.4 mm) was measured usingby the Transient Release and Imbibition method (TRIM) (Lu and Godt, 2013). In this test, the water outflow mass was measured on a 10 minutes basis. In each test, the air pressures of 250 kPa and 0 kPa corresponded to the drying and wetting processes, respectively. Thus, the Soil Water Characteristic Curve (SWCC) and the Hydraulic Conductivity Function (HCF) werewould be obtained by usingthe Hydrus 1-D (Wayllace and Lu, 2012). Using the models proposed by Mualem (1976) and van Genuchten (1980), the constitutive relations between the suction head (h), water content (θ), and hydraulic conductivity (K) under drying and wetting states cancould be represented by the following equation:

$$\frac{\theta-\theta_r}{\theta_s-\theta_r} = \left[\frac{1}{1+(\alpha|h|)^n}\right]^{1-\frac{1}{n}} \qquad (3)$$

and

$$K = K_s \frac{\left\{1-(\alpha|h|)^{n-1}[1+(\alpha|h|)^n]^{\frac{1}{n}-1}\right\}^2}{[1+(\alpha|h|)^n]^{\frac{1}{2}-\frac{1}{2n}}} \tag{4}$$

where θ_r is the residual moisture content (%)~~, %~~,~~;~~ θ_s is the saturated moisture content (%)~~, %~~,~~;~~ α and n are empirical fitting parameters,~~ with~~ α is~~being~~ the inverse of the air-entry pressure head,~~ and~~ n is the pore size distribution parameter, and~~;~~ K_s is the saturated hydraulic conductivity (cm/s)~~, cm/s~~.

The soil water storage (S_s) and drainage (S_d) during a rainfall event can be evaluated by the soil depth and the difference between the maximum soil moisture and ~~the ~~antecedent soil moisture:

$$S_e = \frac{\theta - \theta_r}{\theta_s - \theta_r} \tag{5}$$

$$S_s = S_e^w \Delta h \tag{6}$$

$$S_d = P - S_e^d \Delta h \tag{7}$$

where S_e is the degree of saturation~~ degree~~,~~;~~ θ is the ~~measured ~~volumetric moisture content measured (%)~~, %~~,~~;~~ Δh is the average soil thickness~~, mm~~ (400 mm in this study~~work~~),~~;~~ S_e^w and S_e^d are the residual soil moisture in the wetting and drying processes (%)~~, %~~, and~~;~~ P is the accumulated rainfall (mm)~~, mm~~.

3.4 Stability fluctuation

In this study~~work~~, we applied a finite and infinite stability model to assess the ~~the ~~slope stability fluctuation during the rainy season~~,~~ as an attempt to examine ~~the ~~aspect-dependent landslide initiation from~~by~~ the perspective of classical mechanics and the state of stress (Schmidt et al., 2001). The finite~~-~~-slope model evaluates the stability F_s:

$$F_s = \frac{S_{sr}}{\tau} = \frac{c_l A_l + c_b A_b + A_b(\rho_s - \rho_\omega S_e)\,\mathrm{g}z\cos^2\beta\tan\varphi'}{A_b \rho_s g z \sin\beta\cos\beta} \tag{8}$$

where β is the topographic slope angle (°)~~, °~~,~~;~~ A_l is the lateral area, m^2,~~;~~ A_b is the basal area, m^2,~~;~~ z is the sliding depth (m)~~, m~~,~~;~~ c_l is the sum of the effective soil cohesion and the root additional cohesion along the perimeter (kPa)~~, kPa~~,~~;~~ c_b is the basal soil cohesion (kPa)~~, kPa~~,~~;~~ ρ_s is the soil particle density, g/cm^3, and~~;~~ ρ_w is the water density, g/cm^3.

The infinite slope stability model in this study~~work~~ provides insight into the stress variation resulting from changes in the soil suction and water content during infiltration (Lu and Likos, 2006):

$$F_s = \frac{\tan\varphi'}{\tan\beta} + \frac{2c'}{\gamma z\sin 2\beta} - \frac{\sigma^s}{\gamma z}(\tan\beta + \cot\beta)\tan\varphi' \tag{9}$$

where φ' is the effective friction angle, °; β is the topographic slope angle, °; c' is the effective cohesion, kPa; γ is the unit weight of the soil, KN/m^3; and σ^s is the suction stress (kPa),~~ and~~ expressed as:

$$\sigma^s = -\frac{S_e}{\alpha}\left(S_e^{n/(1-n)} - 1\right)^{1/n} \tag{10}$$

4 Results

4.1 Shallow landslides on south- and north-facing slope

In the study area, the south-facing slope wa~~i~~s between 157.5 ° and 247.5 ° and~~,~~ the north-facing slope ranged~~s~~ from 0 ° to 67.5 °, and 292.5 ° to 360 ° (0 ° is the due north). There were 71 shallow landslides on the south-facing slope~~,~~ and~~while~~ ~~onmerely ~~20 landslides on the north-facing slope. Figure 2a shows~~indicates~~ that ~~the ~~shallow landslides on south-facing slopes have ~~exhibit ~~larger spatial areas than those on north-facing slopes. ~~TheMeanwhile, majority of ~~Most of the shallow landslides occurred~~weare~~ on the south-facing slope (Fig. 2b). ~~Furthermore, T~~the volume of landslides on the south-facing slope was~~is~~ g~~a~~reat~~-ov~~er than that~~ese~~ on the north-facing slope. For landslides on the south-facing slope, the basal area wa~~i~~s 372.64 m^2 and the width wa~~i~~s 14.9 m on average. For landslides on the north-facing slope, the averaged basal area was is merely 157.28 m^2 and the width wasis 7.7 m (Fig. 2c). AltThough the landslides on the south-facing slope hadve a larger volume and greaterwider width, the depth of the head-scar and the sidewall area are no greater than those on the more than the landslides on north-facing slope. Field studies showed investigation reveals that the averaged depth for landslides on the north-facing slope wasis 1.02 m, which wasis deeper than the depth of 0.83 m for landslides on south-facing slope (Fig. 2d). The lLIn all, landslides on the south-facing slope exhibited an overwhelming propensity for occurrence in terms of number and area.., Meanwhile, the failure depth wasis no more than that of the landslides on the north-facing slope.

Shallow landslides can be modelled as occurring when sufficient through-flow converges from the upslope contribution area to the hollow area and triggers slope instability (Montgomery and Dietrich, 1994). Their topographic initiation conditions arecondition is controlled by the spatial competition between the slope and upslope contribution being area dependent (Stock and Dietrich 2003 and 2006; Horton et al., 2008). For the shallow landslides in the study area, the averaged upslope contributing area and the slope gradient did not differ significantly differdo not differentiate a lot (Fig. 3a)., Meanwhile,while the lower limit line representing the minimum initiation condition forof landslides on south-facing slopes wais lower than that on the north-facing slopes (Fig. 3b). This indicates that a higher upslope contributioncontributing area wasis required to provide sufficient through-flow conditions and trigger slope failures on the north-facing slope. Given thatAs the landslides in the study area were triggered by the prolonged antecedent precipitation and intensive rainfall (Li et al., 2021), sufficient rainfall infiltration could result in a high soil water content within the displaced mass, leading to a decrease inof the matricx suction and soil strength. The generation of pore pressure generation in response to intense rainfall also plays an important role in shallow landslides. Therefore, we have proposed two assumptions to elucidate the distribution and scale of the aspect-dependent landslides distribution and scale. The first assumption is that the basal area of the landslide may be related to the soil strength and the high pore-water pressure. This assumption can be tested by the pore water properties, including the pore water generation potential and dissipation ratio, during the failureing process. The second assumption is that the south-facing slope may have a relatively higher failure potential than the north-facing slope in a given rainfall process., which This can be determined elucidated fromby the stability comparison using the methods of equations (8) and (9).

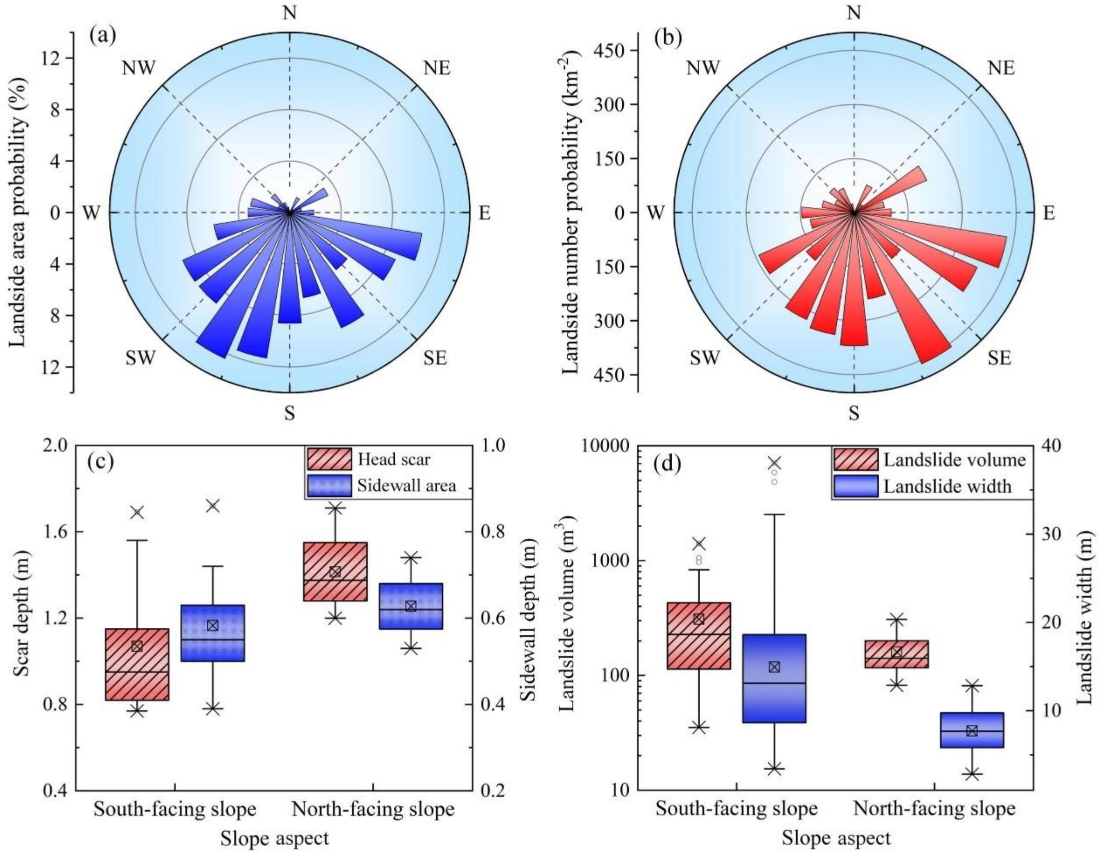

Fig. 2. Spatial distribution and geometric characteristics of the landslide: (a) Landslide area probability vs slope aspect;~~,~~ (b) landslide number probability vs slope aspect;~~,~~ (c) landslide volume and width vs slope aspect;~~,~~ (d) scar depth and sidewall depth vs slope aspect. T~~(t~~he edge line of “~~"~~box”~~"~~ in the box chart shows the 75th quantile, median and 25th quantile from top to bottom. The length of the box is referred to as~~called~~ the inter-quartile distance. The crossed square inside the box is the average value. The whiskers extend to the maximum and minimum values except the outliers. The circles are~~is~~ the outliers, and the cross symbol is the maximum and minimum values for~~of~~ all the data~~)~~.

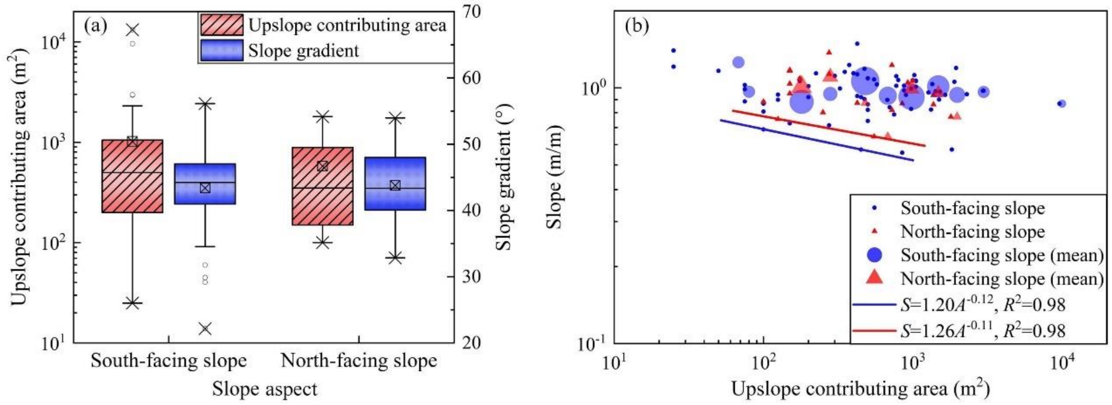

Fig. 3. Upslope contributing area and slope gradient condition: (a) U~~u~~pslope contribution area and mean slope vs slope aspect; and~~,~~ (b) the upslope contributing area vs mean slope gradient above the landslide area. ~~(~~The large icons are the average value with the radius size proportional to the number of landslides. The small icons represent all the individual data values~~)~~.

4.2 Differences in soil physical properties

To show~~reveal~~ the differences in the physical properties of the hillslope materials, the dry unit weights, porosity, and grain size distribution of the soil mass in~~at~~ the three layers on~~of~~ each slope were ~~firstly~~ compared (Fig. 4). The~~n,~~ ~~the~~ effective cohesion and inner friction angle were then examined with respect to the particle component (Table 1 and F~~f~~ig. 5).

Table 1 Physical properties and strength parameters of the soil mass

Parameters	South-facing slope			North-facing slope		
	Layer 1	Layer 2	Layer 3	Layer 1	Layer 2	Layer 3
Unit weight of soil (kN/m^3)	14.8	15.6	17.2	14	16.6	17.1
Porosity (%)	43.0	43.1	36.2	42.5	37.3	36.4
Effective cohesion (kPa)	6.5	17.5	21.2	5.3	9.1	7.9
Effective inner friction angle (°)	29.8	25	31	27.1	35.2	41
Saturated hydraulic conductivity (cm/s)	6.4×10^{-3}	6.2×10^{-4}	4.4×10^{-4}	8.8×10^{-3}	1.2×10^{-3}	4.3×10^{-3}

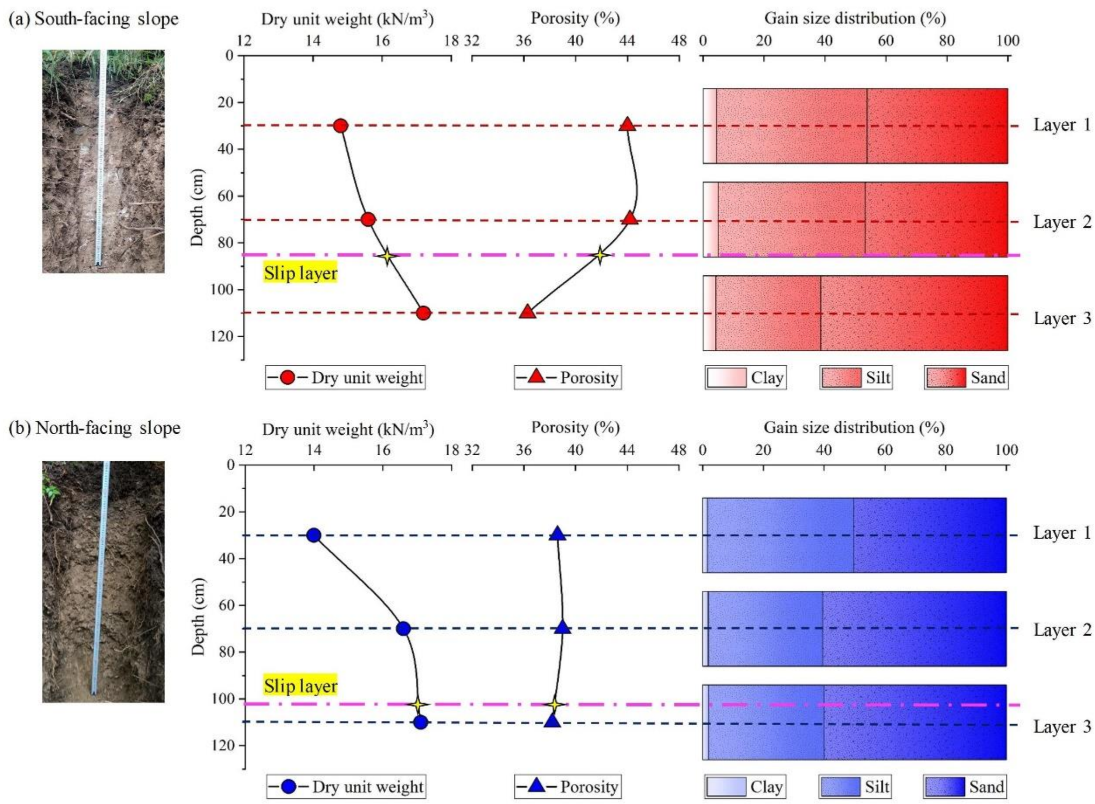

Fig. 4. Differences in the soil properties~~,~~ including dry unit weights, porosity, and grain size in sand, silt, and clay.~~:~~ (a) P~~p~~hysical properties of soil mass on the south-facing slope; and~~,~~ (b) physical properties of soil mass on the north-facing slope. ~~(~~The two-soil profile photos were taken by Yanglin Guo during field studies ~~investigations.)~~

For the soil mass on the south-facing slope, the dry unit weights increased with~~as~~ soil depth, whereas~~while~~ the porosity and saturated hydraulic conductivity decreased (Fig. 4a and T~~t~~able 1). For ~~the~~ S~~s~~oil layers ~~No.~~ 1 and 2, the soil textures were~~is~~ similar, because~~as~~ the proportions of sand, silt, and clay did not differ significantly~~do not differentiate a lot~~. However, the proportion of silt in~~at~~ ~~the~~ S~~s~~oil layer No. 3 wa~~i~~s no more than tha~~te~~ in layers No. 1 and 2, and the sand proportion wa~~i~~s higher. ~~In additionBesides,~~ T~~t~~he average~~d~~ failure depth was~~is~~ above ~~the~~ S~~s~~oil L~~l~~ayer No. 3 and ~~is~~ below ~~the~~ Soil L~~l~~ayer No. 2. For the soil mass on the north-facing slope, the dry unit weight~~s~~

also increased withas soil depth. Unlike the south-facing slope, the porosity of the soil mass for the three soil layers wais approximatelyabout 38% and didoes not differentiate among them. For the the soil texture, the proportion of sand inat Soil Llayer No. 1 wais no more than thate in Soil Llayers No. 2 and 3 (Fig. 4b). MoreoverBesides, Tthe depth of the failure plane wais close to thate of Ssoil Llayer No. 3.

In comparison, one of the main noticeable differences wasis the higher saturated hydraulic conductivity for the soil mass above the failure plane on the north-facing slope., Thiswhich may have resulted from the high porosity and sand proportion. This indicates that the rainfall infiltration on of the north-facing slope could penetrate faster than that of the south-facing slope. Indeed, Tthe soil mass of the three layers on the south-facing slope hadve a relatively higher proportion of fine particles proportion than those on the north-facing slope, if the gravel wais considered (Fig. 5). As noted above, Tthe saturated hydraulic conductivity for the soil masses from Soil of Llayers No. 2 and 3 on the south-facing slope wais lower than that on the north-facing slope. This is expected reasonable because the porosity and proportions of fines on the south-facing slope wereis relatively higher.

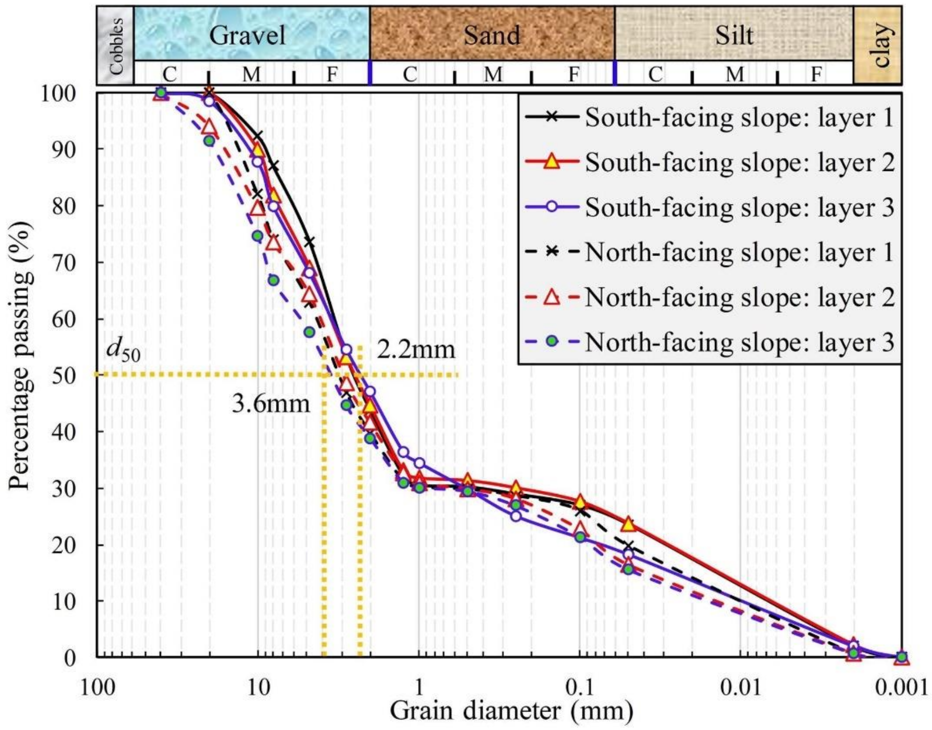

Fig. 5. Soil particle component curves

According to the results of the triaxial shear test (Table 1), the soil mass in each layer on the nNorth-facing slope hads a smaller effective cohesion than that oncomparing to the south-facing slope. In particular, Tthe effective cohesion on the failure plane for landslides on the the south-facing slopes may be twicetwo times of than that on the north-facing slopes. However, the effective inner friction angles for the soil masses of Soil Llayers No. 2 and 3 on the north-facing slope weare far greatermore than those on the south-facing slope. TheseSuch differences in effective cohesion and inner frictional angle may be attributed to the higher clay and silt and fewerless coarse grains within the soil mass on the south-facing slope.

4.3 Pore -water pressure propertiesy

The consolidation module of the triaxial shear test wais used to measure the generation and dissipation process of the pore water pressure. The principle is to consolidate and drain the soil from the initial saturated state. It wais found that Uunder the same confining pressure, there are pronounced obvious differences in the consolidation rate, consolidation time, and peak rise inof pore water pressure foref different soil properties of soil. The results of the pore water pressure during the consolidation process under 200 kPa effective confining pressure were taken here

(Fig. 6). The~~It was found that the~~ peak value of pore water pressure within the soil mass on the south-facing slope was higher than that on the north-facing slope. The peak value of the pore water pressure within the soil mass on the south-facing slope increased~~could rise~~ to 150–~~-~~200 kPa. However, the peak value of pore water pressure within the soil mass on the north-facing slope was below 150 kPa. ~~Importantly, ~~B~~b~~oth ~~of ~~the rising and decaying rates of pore water pressure for S~~s~~oil M~~m~~ass layers ~~No. ~~1 and 2 on the south-facing slope were lower than those~~at~~ on the north-facing slope. ~~. In detail, ~~T~~t~~he ~~rising ~~rate and decaying rates for ~~the ~~S~~s~~oil M~~m~~ass layer No. 2 on the south-facing slope were 1.2 kPa/10 s and −~~-~~0.031 kPa/10 s, respectively. However, they ~~are were~~were 9.6 kPa/10 s and −~~-~~0.765 kPa/10 s for the soil mass on the north-facing slope.

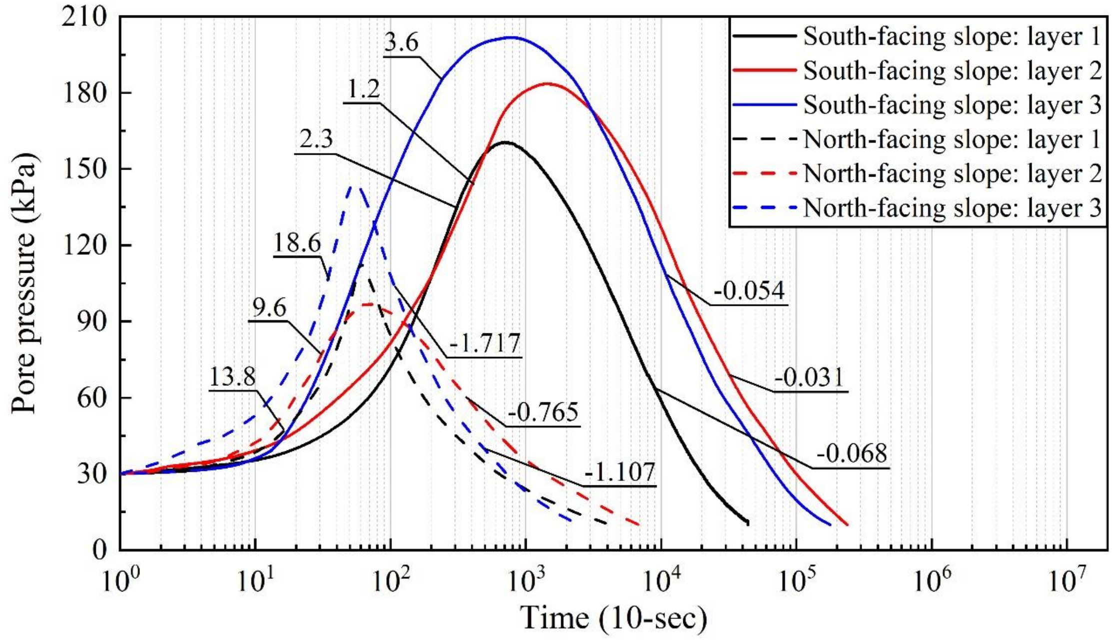

Fig. 6. Variation in~~of~~ pore water pressure under effective confining pressure of 200 kPa by GDS triaxial shear tests.

~~In fact, ~~T~~th~~he~~e~~ ~~relatively ~~lower peak pore water pressure demonstrates ~~can illustrates ~~the effect of fine particles on the pore water pressure, which directly affects ~~the ~~landslide mobility and ~~the ~~scale. ~~It is generally believed that the ~~R~~r~~ainfall-induced landslides result~~s~~ from an increase in~~of~~ positive pore water pressure within the failure plane, which reduces the effective stress and~~in the soil and the~~ shear strength of the soil (Terzaghi, 1950). This often occurs in the undrained soil layer, which can easily~~is easy to~~ cause slope liquefaction (Sassa, 1984). The increase in~~of~~ pore water pressure predominantly ~~mainly ~~depends ~~mainly ~~on the speed of landslide movement, soil deformation, and soil permeability. If the shear rate is ~~the ~~given, the dissipation rate of pore water pressure for high-~~-~~permeability soil is faster, and therefore ~~thus,so~~ the increase in~~of~~ pore pressure is smaller (Iverson and LaHusen, 1989; Iverson et al., 1997). As shown in T~~t~~able 1, the saturated hydraulic conductivity for S~~s~~oil M~~m~~ass L~~l~~ayers No. 2 and 3 on the north-facing slope was~~north-facing slope are commonly~~ 10 times that of the~~at~~ ~~on ~~south-facing slope. Therefore, the ~~measured ~~peak pore water pressure measured during the test for the soil mass on the south-facing slope was~~would be~~ smaller. ~~In additionBesides, ~~T~~t~~he soil mass on the north-facing slope had~~s~~ ~~relatively ~~higher sand and gravel~~s~~ contents than that on the south-facing slope (Fig. 5). A h~~H~~igh clay content on the south-facing slope ~~would ~~filled the macropores within the soil mass and reduced the pore water discharge rate~~ of pore water~~. Wang and Sassa (2003) found that fine particles play the most important role in the dissipation of pore pressure. The pore water pressure within the saturated sand ~~will ~~increased with ~~the ~~shear rate. The soil mass with high coarse particles ~~will ~~produced less pore water pressure than the soil with high fine particles during the shear process. Therefore, the high permeability of~~for~~ the soil mass on the south-facing slope may result in ~~relatively ~~low peak pore water pressure. The relatively higher fine particles may result in a slow increaserising and dissipation of the pore water pressure. ThisSuch slow pore water pressure dissipation could result in the liquefaction failure of the sliding mass and a relatively larger landslide area.

4.4 Unsaturated hydraulic conductivity

4.4.1 Measured water outflow mass

Figure 7 shows the measured water outflow mass measured forin a given 10 min periodminutes during the drying and wetting processes. The measured water outflow masses measured for Soil of Llayers No. 2 and 3 on the north-facing slope weare generally higher than those on the south-facing slope. For the drying tests using the soil mass of Soil Llayers No. 2 and 3 on the north-facing slope, the given water outflow masses weare 0.102 g/10 -min and 0.131 g/10 -min, respectively. However, the measured water outflow masses measured for the soil mass of Soil Layers No. 2 and 3 weare 0.077 g/10 -min and 0.050 g/10 -min, respectively, on the south-facing slope, respectively (Fig. 7a). For tests using the same layers of the soil mass in the wetting process, the measured water outflow masses measured weare 0.051 g/10 -min and 0.094 g/10 -min on the north-facing slope, respectively, andwhile those are 0.032 g/10 -min and 0.027 g/10 -min, respectively, on the south-facing slope -(Fig. 7b). OverallAs a whole, the permeability of the soil mass on the north-facing slope wais higherbetter than that on the south-facing slope. The same results were also obtained when the saturated hydraulic conductivities of the soil layers were measured usingby the constant water head method (Table 1).

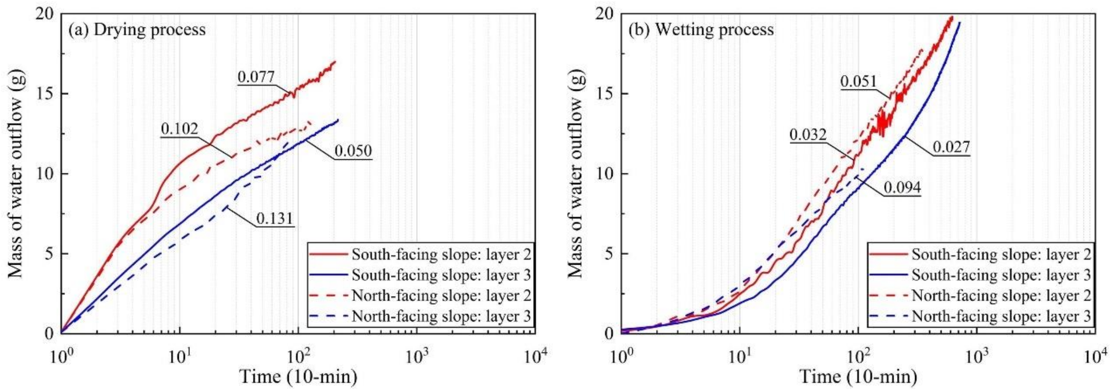

Fig. 7. Mass of water outflow during the drying and wetting process: (a) drying tests, (b) wetting tests.

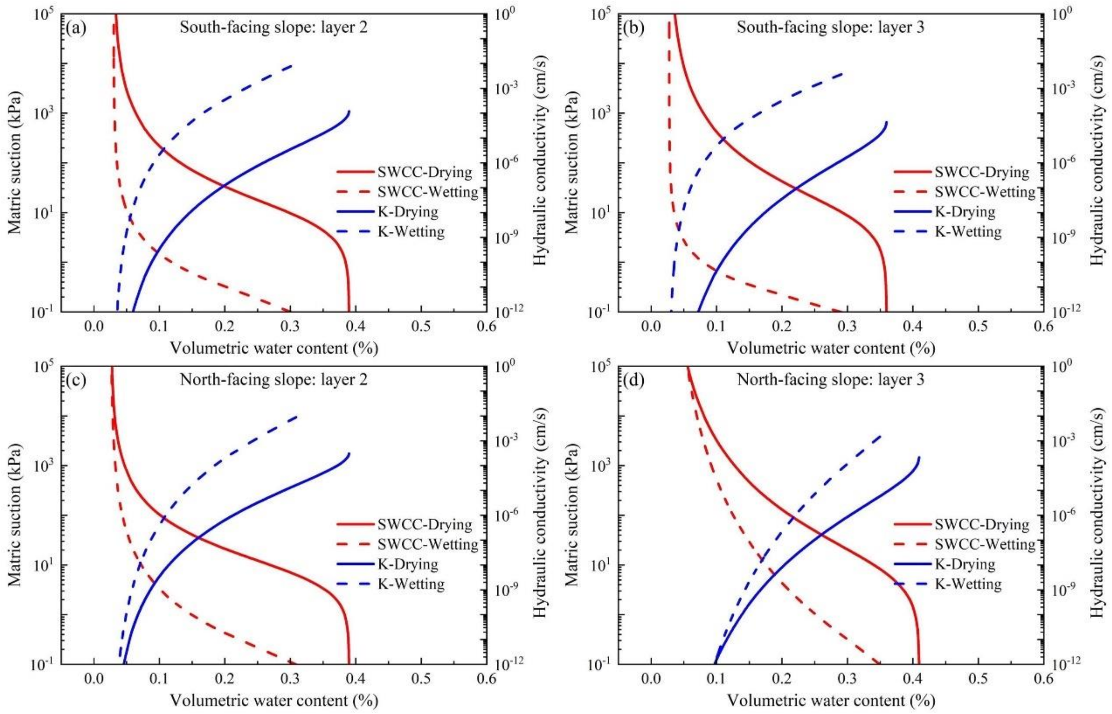

Fig. 8. Soil water ~~characteristic~~ curve obtained using the~~by~~ TRIM test: (a) L~~l~~ayer No. 2 on the south-facing slope, (b) L~~l~~ayer No. 3 on the south-facing slope, (c) L~~l~~ayer No. 2 on the north-facing slope, and (d) L~~l~~ayer No. 3 on the north-facing slope.

4.4.2 SWCC and HCF curves

H~~The h~~ydraulic properties~~,~~ such as the Soil Water Characteristic Curve (SWCC) and Hydraulic Conductivity Function (HCF), are critical for~~to~~ the analysis of water flow movement and mechanical behavior of unsaturated soil material. In this study, ~~the unsaturated hydraulic property measurement adopted~~ the Transient Release and Imbibition Method (TRIM) for unsaturated hydraulic property measurement. The ~~intelligent~~ advantage of the TRIM method is~~TRIM method lies in~~ that it combines physical and numerical experiments. It~~In detail, it~~ employs a~~the~~ relatively simple and reliable measurement of transient water content using an~~by~~ electronic balance to record the signature of transient unsaturated flow.~~,~~ It also~~and~~ takes advantage of the robust inverse modeling capability to simulate the physical process. The apparatus could~~can~~ accommodate both undisturbed and remolded samples. The results of this study were obtained ~~by~~ using the Hydrus-1D code with the reverse modeling option, ~~which implemented~~and ~~–~~the Levenberg–Marquardt non-linear optimization algorithm.~~,~~ This~~and~~ minimized the error between the results of~~in~~ the test and the simulation (Wayllace and Lu, 2012). Meanwhile, ~~in order~~ to ensure the uniqueness of the parameters, the ~~aforementioned~~ algorithm repeatedly runs~~uns~~ with different initial parameter estimates~~,~~ until it ~~always~~ converges to obtain the same or similar results. The~~Compare the~~ prediction results are then compared with the function curves of water flow and time obtained from the actual experiment~~,~~ so that they can be ~~basically~~ combined to meet certain accuracy requirements. In this experiment, the R square of the regression between the optimized predicted value and the observed value wa~~i~~s greater than 0.99. ~~In addition,~~ T~~t~~he model constraint effect of the TRIM~~trim~~ under two suction increment steps wa~~i~~s better, and the parameters obtained by the inversion calculation we~~a~~re more accurate (Lu and Godt, 2013). Table 2 shows the soil ~~characteristic~~ parameters obtained using~~by~~ the Hydrus 1-D inversion.

Using these parameters, the SWCC and HCF curves of the soil mass at S~~s~~oil L~~l~~ayers~~ No.~~ 2 and 3 on the north- and south-facing slopes can be drawn (Fig. 8). A~~The a~~ir-entry pressure~~s~~ and residual water content are two important parameters that describe~~ing~~ the hydrological and mechanical characteristics of the hillslope materials. The air-entry pressure~~s~~ represent~~s~~ the critical value at which~~en~~ air enters the saturated soil and starts to drain. For ~~the~~ S~~s~~oil L~~l~~ayer No. 2, the difference between the air ~~-~~entry values of the north- and south-facing slopes can reach 14.03 kPa (Figs. 8a and 8c). ~~In additionBesides,~~ T~~t~~he residual water content~~s~~ and air-entry pressure~~s~~ of the south-facing slope we~~a~~re higher than those of the north-facing slope. For ~~the~~ S~~s~~oil L~~l~~ayer No. 3, the soil mass on the north-facing slope has the smallest air-entry pressure, which is 0.51 times that of the air-entry pressure of the south-facing slope (Figs. 8b and 8d). The saturated hydraulic conductivities of S~~s~~oil L~~l~~ayers No. 2 and 3 on the south-facing slope we~~a~~re lower than those on the north-facing slope in both the drying and wetting processes. ~~In particular,~~ T~~t~~he saturated hydraulic conductivity of the soil mass on the north-facing slope in the wetting test wa~~i~~s one order of magnitude higher than that on the south-facing slope. These results suggest~~imply~~ that it is more difficult for the soil mass ~~the soil mass on south-facing slope is more difficult~~ to absorb ~~water~~ and drain water than the soil mass on the north-facing slope.

Table 2 Parameters describing the Soil and Water Characteristic Curve (SWCC) and the Hydraulic Conductivity Function (HCF) from~~by~~ Hydrus 1-D

Parameters	Definition	South-facing slope		North-facing slope	
		Layer 2	Layer 3	Layer 2	Layer 3
θr	Residual moisture	0.0302	0.0278	0.0262	0.0268
θs^d	Saturated moisture	0.39	0.36	0.39	0.41
θs^w		0.36	0.38	0.39	0.42
α^d (kPa^{-1})	The inverse of the air-entry pressure head	0.0128	0.0117	0.0156	0.0141
α^w (kPa^{-1})		0.78	0.94	1.21	1.86
n^d	The pore size distribution parameter	1.49	1.39	1.57	1.27
n^w		1.63	1.85	1.43	1.18
K_s^d (cm/s)	Saturated hydraulic conductivity	1.52×10^{-4}	0.64×10^{-4}	3.76×10^{-4}	4.56×10^{-4}
K_s^w (cm/s)		9.58×10^{-2}	4.93×10^{-2}	4.10×10^{-1}	4.68×10^{-1}

Notes: the superscript *d* and *w* indicate drying and wetting states.

4.5 Water storage and drainage

To show~~exhibit~~ the water storage during the rainfall process and the water drainage after the rainfall, the timely ~~-~~recorded soil moisture at vari~~used~~ous soil layers and the rainfall process during June 11 and August 20 were used (Figs. 9a and 9b). In comparison, this~~it~~ is likely the most important~~significant~~ finding, as it shows that the soil becomes nearly saturated on the south slope, but~~while~~ not on the north slope. This implies that the soil water on the south-facing slope has~~is~~ difficulty in ~~to~~ draining because of the presence of more fine grains and ~~the~~ slow pore water pressure dissipation. ~~In additionBesides,~~ T~~t~~he stable soil moisture from~~of~~ Soil L~~l~~ayers No. 2 and 3 for both slopes may be attributed to the long dry seasons in the study area. ~~, Tand t~~he daily rainfall amount > 30 mm on July 9 and 23 resulted in an increase in soil moisture ~~increase~~ for all the slope layers.

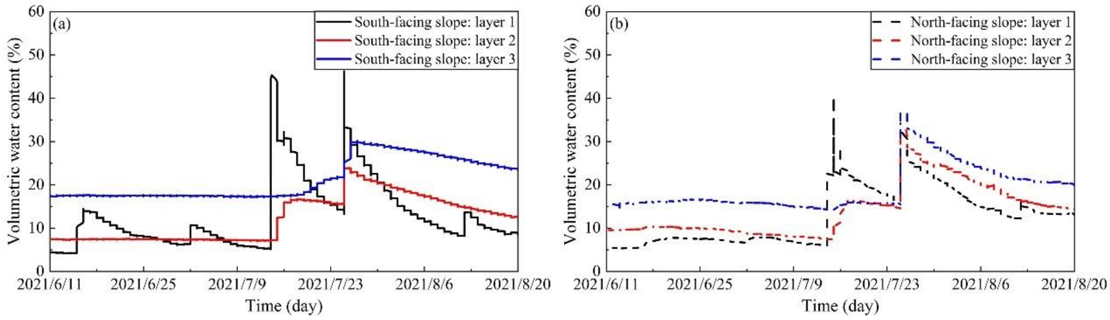

Fig. 9. Field monitored volumetric water content: (a) S~~s~~oil moisture on the south-facing slope, and (b) soil moisture on the north-facing slope.

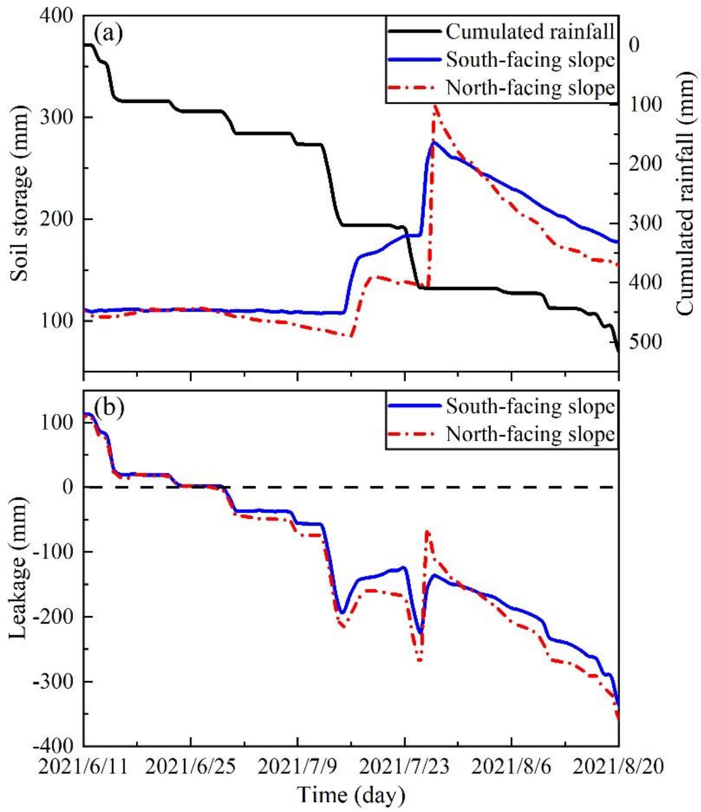

Fig. 10. Seepage model of slope water storage and drainage.~~:~~ (a) soil water storage, (b) soil water drainage

~~It can be seen from~~ Fig. 10a shows that the storied water of the north- and south-facing slopes did~~does~~ not synchronously increase with ~~the~~ accumulated precipitation. When the storied water rapidly increase~~ds rapidly~~, the increase in~~of~~ ~~the~~ soil water storage of the north-facing slope wa~~i~~s greater~~larger~~ than that of the south-facing slope. On July 26, a rainfall of 30.8 mm/h was recorded~~occurred~~, and the water storage of the slope reached the peak. ~~It can be seen that~~ T~~t~~he~~he~~ peak of the water storage on~~of~~ the north-facing slope was~~is~~ higher than that of the south-facing slope. However, when the accumulated rainfall tends to be stable, that is, when the rainfall stops for a period of time, the decline rate of the soil water storage on the north-facing slope is substantially~~much~~ higher than that on the south-facing slope. ~~In general,~~ T~~t~~he soil water storage of the south-facing slope wa~~i~~s always higher than that of the north-facing slope during ~~the~~ rainfall~~ process~~. During~~In~~ the ~~process of~~ drainage process, the seepage rate of the north-facing slope wa~~i~~s greater than that of the south-facing slope (Fig. 10b). Therefore, the south-facing slope had~~s~~ a better water storage performance, and the north-facing slope had~~s~~ a higher drainage performance.

4.6 Stability fluctuation

In this study, the infinite slope model and the finite slope model we~~a~~re used to characterize the sensitivity of landslide triggering~~,~~ in~~so~~ order~~as~~ to determine the main mechanism of high ~~overwhelming~~ landslide probability on south-facing slopes~~s~~. The infinite slope model can be used to examine~~studies~~ the transient stress changes caused by water entering the soil, emphasizing the differences in~~of~~ soil permeability (Lu and Likos, 2006; Lu and Godt, 2013). The finite slope model focuses on the cohesion of the base surface and lateral periphery of the ground landslide source body, as well as the influence of~~of~~ the ~~lateral~~ additional lateral cohesion provided by the vegetation root system for the landslide (Schmidt et al., 2001; Dai et al., 2022).

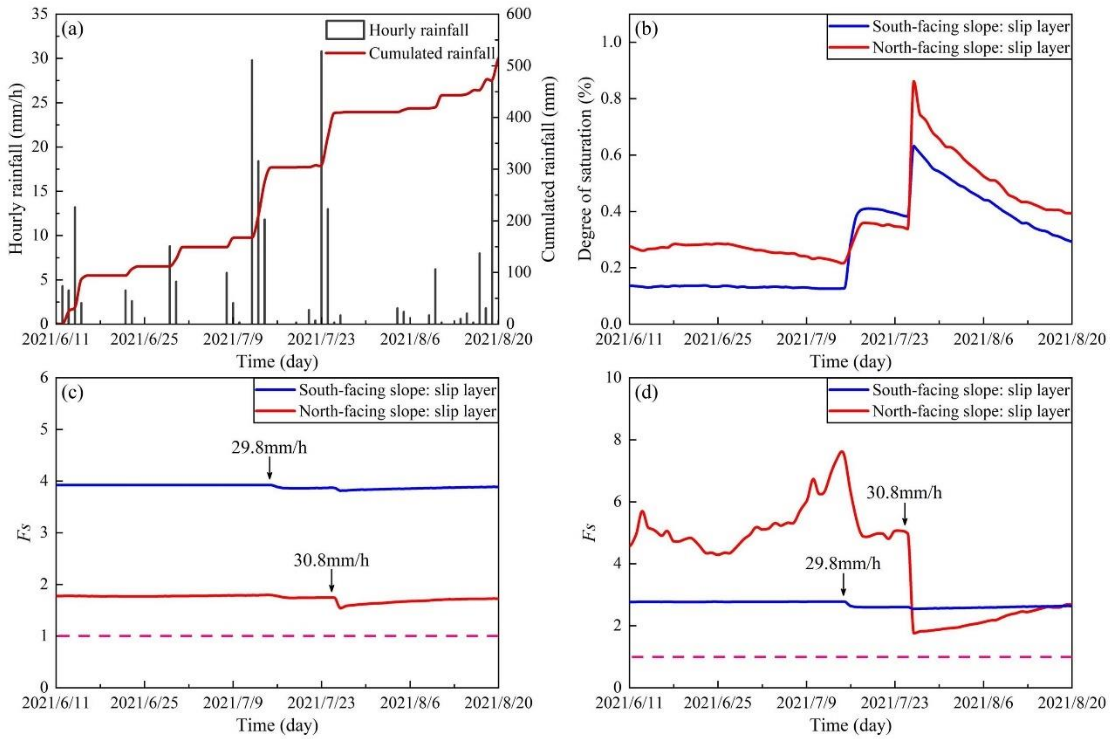

Fig. 11. Change in~~of~~ slope stability fluctuation: (a) rainfall records, (b) degree of saturation, (c) stability of finite slope model, and (d) stability of infinite slope model.

Figure 11a shows the rainfall records from June 11 to August 20, 2021. In general, ~~t~~the degree of saturation ~~degree~~ of the sliding layer on~~f~~ the south-facing slope was higher than that on the north-facing slope (Fig. 11b). In the finite model, the stability of the south-facing slope was always higher than that of the north-facing slope (Fig. 11c). In the infinite model, the stability of the north-facing slope was generally higher than that of the south-facing slope, and the stability of the north-facing slope fluctuated substantially ~~significantlygreatly~~ (Fig. 11d). On July 26, a rainfall event with a maximum intensity of 30.8 mm/h resulted in a sudden decrease in~~of~~ stability. ~~More importantly,~~ T~~t~~he estimated stability index of the north-facing slope decreased~~s~~ to become lower than that of the south-facing slope~~,~~ and then~~while~~ increased afterwards. Although the soil moisture of the south-facing slope increased substantially ~~significantly increased~~ during the rainfall event on July 16, the stability fluctuation was relatively~~veryso~~ small.~~,~~ This may~~which~~ ~~might~~ be related to the relatively strong effective cohesion and smaller pore structure. ~~In~~ Overall, the results of the finite slope model have shown ~~reveal~~ that the south-facing slope has a relatively high stability.~~,~~ This~~which~~ is predominantly ~~mainly~~ attributed to the ~~fact that the~~ effective cohesion of hillslope materials on the south-facing slope being~~is~~ stronger than that of~~n~~ the north-facing slope although~~,~~ ~~even though~~ the basal area of the landslide is more than double~~twice~~. However, this result is inconsistent with the high ~~overwhelming~~ landslide density on the south-facing slopes. ~~The rResults of the infinite slope model,~~ C~~c~~onsidering the soil ~~characteristic~~ parameters of the soil moisture ~~characteristic~~ curve, the results of the infinite slope model have shown ~~revealed~~ that the north-facing slope showed~~s~~ a higher level of stability. In the analysis of finite and infinite models, the stability fluctuation amplitude of the south-facing hillslope wa~~i~~s smaller than that of the north-facing hillslope This indicated~~,~~ ~~indicating~~ that the water movement on~~in~~ the south-facing slope wa~~i~~s less active than that of~~in~~ the north-facing slope. Therefore, in the~~is~~ study area, the change in~~of~~ soil stress wa~~i~~s more sensitive to ~~the~~ slope stability than the change in~~of~~ root soil cohesion. ~~It wais verified that~~ T~~t~~he change in~~of~~ soil permeability caused by ~~the~~ differential weathering of the bedrock could be responsible for ~~the~~ aspect-dependent landslide initiation in the study area.

5 Discussion

The ~~landslide~~ strong~~overwhelming~~ propensity for landslides in some arid environments in the Northern H~~h~~emisphere is~~are~~ scientifically interesting, and some researchers~~scholars~~ have highlighted the contribution of plant roots. This~~Such a~~ finding is to ~~would~~ be expected in the future in other mountain regions, where water is a limiting~~ed~~ factor for local system sustainability. In the Colorado Frontal range, McGuire et al. (2016) found that the apparent cohesion supplied by roots was responsible for the ~~observed~~ connection observed between landslide distribution and slope aspect (Ebel, 2015; Rengers et al., 2016). In the study area, Li et al. (2021) also found that ~~the~~ plant roots may explain the ~~observed~~ connection observed between vegetation cover and landslide probability for the entire~~whole~~ study area. ~~Furthermore,~~ Dai et al. (2022) found that a strong root network and high saturated hydraulic conductivity may promote the *A*–~~-~~*S* condition of shallow landslides. On~~In~~ the ~~the~~ Loess Plateau in China, some ~~scholars~~ researchers have observed that the strong ~~overwhelming~~ propensity for shallow landslide initiation is closely related~~s~~ to the present-day tree density, and plant roots do not penetrate over the failure plane (Guo et al., 2020; Deng et al., 2022). However, the strong ~~overwhelming~~ propensity for~~of~~ shallow landslides on north- and south-facing slopes could not~~n't~~ be attributed to ~~the~~ plant roots, because~~as~~ the artificial ~~man-made~~ vegetation on both slopes is~~are~~ the same. Conversely, these~~such~~ observations could be the result of ~~from~~ the soil hydraulic and mechanical properties from ~~owing to~~ differential weathering.

This study has~~work~~ contributed~~s~~ to ~~the~~ knowledge of~~know about~~ the effect of differential weathering on ~~the~~ aspect-dependent landslide initiation from~~by~~ the perspective of soil hydraulic properties, in addition to~~other than~~ ~~from~~ the mechanical and hydrological effects of plant roots. Except for the strong ~~overwhelming~~ propensity for a high number of~~in~~ landslides~~-number~~, ~~the~~ shallow landslides on south-facing slopes have exhibited ~~relatively~~ larger areas and greater ~~wider~~ widths than those on the north-facing slopes (Fig. 2). The~~In comparison, the~~ effective cohesion of the failure zone on the south-facing slope wa~~i~~s stronger than that on the north-facing slope.~~. It seems that~~ T~~t~~he basal area of shallow landslides in the study area may be attributed to ~~the~~ effective cohesion, because~~as~~ some statistical results have shown ~~reveal~~ that incoherent materials favor shallow landslides with no limitation in size.~~;~~ Meanwhile, cohesive materials favor deep landslides and show a limitation for small sizes (Larsen et al., 2010; Frattini and Crosta, 2013; Milledge et al., 2014). However, a stronger effective cohesion tends to promote the *A*–~~-~~*S* conditions of shallow landslides. ~~In other words,~~ A~~a~~ ~~relatively~~ larger up-slope contributing area or steeper gradient is required to trigger slope failure~~s~~. ~~In fact,~~ F~~f~~ig. 3 shows ~~illustrates~~ that some shallow landslides on south-facing slopes fail i~~o~~n ~~relatively~~ lower upslope contributing areas. Therefore, ~~the~~ soil hydraulic property~~ies~~-related factors, such as the rising or dissipation of pore water pressure, water storage, and drainage, may contribute to the ~~observed~~ phenomena observed.

The saturated hydraulic conductivities obtained by the ~~by~~ constant water head ~~method~~ and TRIM methods coincide~~ with each other~~, which ~~together~~ demonstrates~~proves~~ that the hillslope material on the north-facing slope has a ~~relatively~~ larger water infiltration (Tables 1 and 2). However, the results of the stability analysis using~~by~~ the finite and infinite models imply that the failure potential of slides on a north-facing slope is ~~relatively~~ lower than that~~e~~ on a south-facing slope, although the stability index fluctuates more heavily than the north-facing slope. These~~Such~~ differences imply that slope failures on a north-facing slope may only occur ~~only~~ under intensive rainfall conditions~~on condition of intensive rainfall merely,~~ or by a combination of prolonged antecedent precipitation and short ~~-~~duration intensive rainfall. For potential failures on south-facing slopes, the combination of prolonged antecedent precipitation and short ~~-~~duration intensive rainfall should be a potential~~the possible~~ trigger owing~~due~~ to the low hydraulic conductivity and pore water pressure dissipation. ~~Additionally, T~~This study~~work mainly~~ highlights the role of hydraulic properties i~~o~~n ~~the~~ landslide occurrence. Alt~~T~~hough the south- and north-facing slopes are ~~merely~~ underlain by granite, the physical properties of hillslope materials~~,~~ such as ~~the~~ excessive pore water pressure, strength of sliding mass, soil water storage, and leakage~~,~~ are significantly different~~differentiates a lot~~. ~~Such a~~ This finding cannot be random because the study area has been~~is~~ selected on the condition that it is relatively far from the northern and eastern areas~~,~~ where local soils are predominantly~~mainly~~ ~~from~~ l~~L~~oess deposits, and the study areas of Li et al. (2021) and Dai (2022), where the bedrock underneath differs substantially~~greatly~~. ~~Finally,~~ T~~t~~he~~is~~ main purpose of this work is~~merely~~ to elucidate~~s~~ the reason for~~of~~ ~~the~~ aspect-dependent landslide initiation from~~by~~ the perspective of soil hydraulic properties. These~~Such~~ differences ~~essentially~~ result~~s~~ from ~~the~~ differential weathering owing to the amount of direct sunlight. Other mechanics~~,~~ such as numerical or relative dating methods and~~,~~ preferential flow in the macro~~-~~pore distribution~~,~~ could provide new evidence~~s~~ for~~to~~ such observations.

6 Conclusion

Previous research~~es~~ on~~about~~ the strong ~~overwhelming~~ propensity for~~of~~ shallow landslides on south-facing slopes over north-facing slopes has highlighted the role of plant roots. In a localized area with the same vegetation~~,~~ including ~~especially the~~ plant roots, they do ~~does~~ not penetrate the~~over~~ failure layer.~~;~~ These~~such~~ observations cannot~~could~~ be~~n't~~ attributed to plant roots and may result from the differential weathering of bedrock under the influence of hydrothermal conditions. In this study~~work~~, we jointly explained the influence of bedrock weathering on soil hydraulic properties from physical and mechanical properties, pore water pressure, unsaturated hydraulic conductivity, water storage and drainage, and slope stability fluctuation during monitoring, and studied ~~the~~ landslide initiation related to slope direction. The following conclusions were~~can be~~ drawn:

(1) In terms of soil physical and mechanical properties on both slopes, the soil masses on the south-facing slope we~~a~~re rich in clay content, whereas~~while~~ the soil mass on the north-facing slope had~~s~~ relatively high sand content. The effective cohesion of~~n~~ the soil mass on the south-facing slope wa~~i~~s higher than that on the north-facing slope, while the effective frictional angle wa~~i~~s smaller.

(2) The r~~R~~esults of the GDS tests showed ~~revealed~~ that the dissipation rate of pore water pressure for soil mass on the south-facing slope wa~~i~~s substantially~~much~~ lower than that o~~i~~n the north-facing slope. Higher effective cohesion and ~~the~~ slower pore water pressure dissipation may result in a~~the~~ larger basal area for~~of~~ shallow landslides on south-facing slopes.

(3) The soil mass on the south-facing slope had~~s~~ a higher residual water content and air ~~-~~entry pressure, and a lower saturated hydraulic conductivity than that of~~on~~ the north-facing slope. For ~~the~~ water storage and drainage performance, the storied water from~~of~~ the south-facing slope wa~~i~~s higher than that of the north-facing slope, while the north-facing slope had~~s~~ a higher leakage rate. The r~~R~~esults of the stability analysis based on the~~on basis of~~ finite and infinite models show ~~illustrate~~ that the infinite slope model may be suitable for elucidating ~~the~~ aspect-dependent landslide distribution in the study area.

Acknowledgements

This study was supported by the Fundamental Research Funds for the Central Universities (Grant No. 2018BLCB03), the State Key Program of National Natural Science of China (Grant No. 42130701), and the National Nature Science Foundation of China (42177309). The authors sincerely thank the contributions of~~from~~ other colleges, including Muyang Li, Zhisheng Dai, Lv Miao, Lijuan Wang, and Jiayong Deng, for their previous work near the study area.

Code/Data availability

The raw/processed data in this work cannot be shared at this time, because~~as~~ the data also form~~s~~ part of an ongoing study.

Author contributions

Professor Ma Chao found a strong~~the overwhelming~~ propensity for~~of~~ shallow landslide initiation on south-facing hillslopes in the study area and launched a~~the~~ research proposal. Miss Yanglin Guo completed~~finished~~ the sampling collection and indoor tests.

Competing interests

All authors have declared that there were no conflicts of interests and competing interests.

References

[1] Bierman, P. R., Montgomery, D. R.: Key Concepts in Geomorphology, W.H. Freeman, 2014.

[2] Birkeland, P. W.: Soils and Geomorphology, New York: Oxford University Press, 1999.

[3] Bogaard, T. A., Greco, R.: Landslide hydrology: from hydrology to pore pressure, Wiley Interdiscip. Rev. Water, 3, 439-459, https://doi.org/10.1002/wat2.1126, 2016.

[4] Coe, J. A., Kean, J. W., Godt, J. W., Baum, R. L., Jones, E. S., Gochis, D. J., Anderson, G. S.: New insights into debris-flow hazards from an extraordinary event in the Colorado front range, GSA Today, 24, 4-10, https://doi.org/10.1130/GSATG214A.1, 2014.

[5] Dai, Z. S., Ma, C., Miao, L., Li, M. Y., Wu, J. L. and Wang, X. H.: Initiation conditions of shallow landslides in two man-made forests and back estimation of the possible rainfall threshold, Landslides, 19, 1031-1044, https://doi.org/10.1007/s10346-021-01823-1, 2022.

[6] Deng, J. Y., Ma, C., and Zhang, Y.: Shallow landslide characteristics and its response to vegetation by example of July 2013, extreme rainstorm, Central Loess Plateau, China. Bulletin of Engineering Geology and the Environment, 81-100, https://doi.org/10.1007/s10064-022-02606-1, 2022.

[7] Ebel, B. A., Rengers, F. K., Tucker, G. E.: Aspect-dependent soil saturation and insight into debris-flow initiation during extreme rainfall in the Colorado front range, Geology, 43, 659-662, https://doi.org/10.1130/G36741.1, 2015.

[8] Frattini, P., Crosta, G. B.: The role of material properties and landscape morphology on landslide size distributions, Earth Planet. Sci. Lett., 361, 310-319, https://doi.org/10.1016/j.epsl.2012.10.029, 2013.

[9] Fu, B. J., Wang, Y. F., Lu, Y. H., He, C. S., Chen, L. D., Song, C. J.: The effects of land-use combinations on soil erosion: a case study in the Loess Plateau of China, Prog. Phys. Geo., 33, 793-804, https://doi.org/10.1177/0309133309350264, 2009.

[10] Fu, B. P.: Mountain climate, Science Press, 1983 (in Chinese)

[11] Geroy, I. J., Gribb, M. M., Marshall, H. P., Chandler, D. G., Benner, S. G., McNamara, J. P.: Aspect influences on soil water retention and storage, Hydrological Processes, 25, 3836-3842, https://doi.org/10.1002/hyp.8281, 2011.

[12] Godt, J. W., Baum, R. L., and Lu, N.: Landsliding in partially saturated materials. Geophys. Res. Lett., 36, L02403, https://doi.org/10.1029/2008GL035996, 2009.

[13] Guo, F. Y., Meng, X. Y., Li, Z. H., Xie, Z. T., Chen, G., He, Y. F.: Characteristics and causes of assembled geo-hazards induced by the rainstorm on 25th July 2013 in Tianshui City, Gansu, China, Mt. Res., 33, 100-107, 2015 (in Chinese)

[14] Guo, W. Z., Chen, Z. X., Wang, W. L., Gao, W. W., Guo, M. M., Kang, H. L., Li, P. F., Wang, W. X., Zhao, M.: Telling a different story: The promote role of vegetation in the initiation of shallow landslides during

rainfall on the Chinese Loess Plateau, Geomorphology, 350, 106879, https://doi.org/10.1016/j.geomorph.2019.106879, 2020.

[15] Hungr, O., McDougall, S., Bovis, M.: Entrainment of material by debris flows. In: Debris-flow Hazards and Related Phenomena. Springer Praxis Books. Springer, Berlin, Heidelberg. https://doi.org/10.1007/3-540-27129-5_7, 2005.

[16] Iverson, R. M., LaHusen, R. G.: Dynamic pore-pressure fluctuations in rapidly shearing granular materials, Science, 246, 796-799, https://doi.org/10.1126/science.246.4931.796, 1989.

[17] Iverson, R. M., Reid, M. E., LaHusen, R. G.: Debris-flow mobilization from landslides, Annu. Rev. Earth Planet. Sci., 25, 85-138, https://doi.org/10.1146/annurev.earth.25.1.85, 1997.

[18] Iverson, R.M., Reid. M.E., Logan, M., Lahusen, R.G., Godt, J.W., Griswold, J.P.: Positive feedback and momentum growth during debris-flow entrainment of wet bed sediment, Nature. Geosci., 4(2), 116–121, https://doi.org/10.1038/ngeo1040, 2011.

[19] Larsen, I. J., Montgomery, D. R., Korup, O.: Landslide erosion controlled by hillslope material, Nat. Geosci., 3, 247-251, https://doi.org/10.1038/ngeo776, 2010.

[20] Lee, E., Kim, S. Seasonal and spatial characterization of soil moisture and soil water tension in a steep hillslope, J. Hydrol., 568, 676-685, https://doi.org/10.1016/j.jhydrol.2018.11.027, 2019.

[21] Li, M. Y., Ma, C., Du, C., Yang, W. T., Lyu, L. Q., Wang, X. H.: Landslide response to vegetation by example of July 25-26, 2013, extreme rainstorm, Tianshui, Gansu Province, China, Bull. Eng. Geol. Environ., 80, 751-764, https://doi.org/10.1016/10.1007/s10064-020-02000-9, 2021.

[22] Lu, N., and Godt. J. W.: Hillslope hydrology and stability, Cambridge Univ. Press, Cambridge, UK, 2013.

[23] Lu, N., and Likos, W. J.: Suction stress characteristic of unsaturated soils, J. Geotech. Geoenviron. Eng., 132, 131-142, http://doi.org/10.1061/(ASCE)1090-0241(2006)132:2(131), 2006.

[24] McGuire, L. A., Rengers, F. K., Kean, J. W., Coe, J. A., Mirus, B. B., Baum, R. L., Godt, J. W.: Elucidating the role of vegetation in the initiation of rainfall-induced shallow landslides: insights from an extreme rainfall event in the Colorado front range, Geophys. Res. Lett., 43, 9084-9092, https://doi.org/10.1002/2016GL070741, 2016.

[25] Milledge, D. G., Bellugi, D., McKean, J. A., Densmore, A. L., Dietrich, W. E.: A multidimensional stability model for predicting shallow landslide size and shape across landscapes, J. Geophys. Res.: Earth Surf., 119, 2481-2504, https://doi.org/10.1002/2014JF003135, 2014.

[26] Montgomery, D. R., Dietrich, W. E.: Landscape dissection and drainage area-slope thresholds, In: Kirkby MJ (ed) Process models and theoretical geomorphology, John Wiley, Hoboken, N. J., pp: 221-246, 1994.

[27] Mualem, Y.: Hysteretical models for prediction of the hydraulic conductivity of unsaturated porous media, Water Resour. Res., 12, 1248-1254, https://doi.org/10.1029/WR012i006p01248, 1976.

[28] Rengers, F. K., McGuire, L. A., Coe, J. A., Kean, J. W., Baum, R. L., Staley, D. M., Godt, J. W.: The influence of vegetation on debris-flow initiation during extreme rainfall in the northern Colorado front range, Geology, 44, 823-826, http://doi.org/10.1130/G38096.1, 2016.

[29] Sassa, K.: The mechanism starting liquefied landslides and debris flows. Proceedings of 4th International Symposium on Landslides, Toronto, Canada, vol. 2, pp. 349-354, 1984.

[30] Schmidt, K. M., Roering, J. J., Stock, J. D., Dietrich, W. E., Montgomery, D. R., Schaub, T.: The variability of root cohesion as an influence on shallow landslide susceptibility in the Oregon Coast Range, Can. Geotech., 38, 995-1024, http://doi.org/10.1139/cgi-38-5-995, 2001.

[31] Schwinning, S.: The ecohydrology of roots in rocks, Ecohydrology: Ecosystems, land and water process interactions, Ecohydrology, 3, 238-245，https://doi.org/10.1002/eco.134，2010.

[32] Terzaghi, K.: Mechanism of landslides. In: Paige, S. (Ed.), Application of Geology to Engineering Practice (Berkey Volume). Geological Society of America, New York, pp. 83-123, 1950.

[33] Timilsina, S., Niemann, J. D., Rathburn, S. L., Rengers, F. K., Nelson, P. A.: Modeling hydrologic processes associated with soil saturation and debris flow initiation during the September 2013 storm, Colorado Front Range, Landslides, 18, 1741-1759, https://doi.org/10.1007/s10346-020-01582-5, 2021.

[34] Van Genuchten, M. T.: A closed-form equation for predicting the hydraulic conductivity of unsaturated soils, Soil Sci. Soc. Am. J, 44, 892-898, https://doi.org/10.2136/sssaj1980.03615995004400050002x, 1980.

[35] Wang, C. Y.: Study on the relationship between aspect and slope stability, Dissertation, Kunming University of Science and Technology, 2008 (in Chinese).

[36] Wang, G. H., Sassa, K.: Pore-pressure generation and movement of rainfall-induced landslides: effects of grain size and fine-particle content, Eng. Geol., 69, 109-125, https://doi.org/10.1016/S0013-7952(02)00268-5, 2003.

[37] Wang, X. H., Ma, C., Wang, Y. Q., Wang, Y. J., Li, T., Dai, Z. S., Li, M. Y.: Effect of root architecture on rainfall threshold for slope stability: variabilities in saturated hydraulic conductivity and strength of root-soil composite, Landslides, 17, 1965-1977, https://doi.org/10.1007/s10346-020-01422-6, 2020.

[38] Watakabe, T., Matsushi, Y.: Lithological controls on hydrological processes that trigger shallow landslides: Observations from granite and hornfels hillslopes in Hiroshima, Japan, Catena, 180: 55-68, https://doi.org/10.1016/j.catena.2019.04.010，2019

[39] Wayllace, A., Lu, N.: A transient water release and imbibitions method for rapidly measuring wetting and drying soil water retention and hydraulic conductivity functions. Geotech. Test. J., 35, 1-15, 2012.

[40] Yu, G. Q., Zhang, M. S., Hu, W.: Analysis on the development characteristics and hydrodynamic conditions for massive debris flow in Tianshui, Northwest Geol., 47, 185-191, 2014 (in Chinese)